

# The use of simultaneous stereo-electroencephalography and magnetoencephalography in localizing the epileptogenic focus in refractory focal epilepsy

Umesh Vivekananda, Chunyan Cao, Wei Liu, Jing Zhang, Fergus Rugg-Gunn, Matthew C Walker, Vladimir Litvak, Bomin Sun, Shikun Zhan



**Accelerating clinical advancements –  
from development to delivery.**

**DISCOVER MORE**

HOUSTON  
**Methodist**  
NEUROLOGICAL INSTITUTE

# BRAIN COMMUNICATIONS

## The use of simultaneous stereo-electroencephalography and magnetoencephalography in localizing the epileptogenic focus in refractory focal epilepsy

 **Umesh Vivekananda,<sup>1,\*</sup> Chunyan Cao,<sup>2,3,\*</sup> Wei Liu,<sup>2</sup> Jing Zhang,<sup>2</sup> Fergus Rugg-Gunn,<sup>1</sup>**  
 **Matthew C. Walker,<sup>1</sup> Vladimir Litvak,<sup>3</sup> Bomin Sun<sup>2</sup> and Shikun Zhan<sup>2</sup>**

\* These authors are joint first author.

Both magnetoencephalography and stereo-electroencephalography are used in presurgical epilepsy assessment, with contrasting advantages and limitations. It is not known whether simultaneous stereo-electroencephalography–magnetoencephalography recording confers an advantage over both individual modalities, in particular whether magnetoencephalography can provide spatial context to epileptiform activity seen on stereo-electroencephalography. Twenty-four adult and paediatric patients who underwent stereo-electroencephalography study for pre-surgical evaluation of drug-resistant focal epilepsy, were recorded using simultaneous stereo-electroencephalography–magnetoencephalography, of which 14 had abnormal interictal activity during recording. The 14 patients were divided into two groups; those with detected superficial ( $n=7$ ) and deep ( $n=7$ ) brain interictal activity. Interictal spikes were independently identified in stereo-electroencephalography and magnetoencephalography. Magnetoencephalography dipoles were derived using a distributed inverse method. There was no significant difference between stereo-electroencephalography and magnetoencephalography in detecting superficial spikes ( $P=0.135$ ) and stereo-electroencephalography was significantly better at detecting deep spikes ( $P=0.002$ ). Mean distance across patients between stereo-electroencephalography channel with highest average spike amplitude and magnetoencephalography dipole was  $20.7 \pm 4.4$  mm. for superficial sources, and  $17.8 \pm 3.7$  mm. for deep sources, even though for some of the latter ( $n=4$ ) no magnetoencephalography spikes were detected and magnetoencephalography dipole was fitted to a stereo-electroencephalography interictal activity triggered average. Removal of magnetoencephalography dipole was associated with 1 year seizure freedom in 6/7 patients with superficial source, and 5/6 patients with deep source. Although stereo-electroencephalography has greater sensitivity in identifying interictal activity from deeper sources, a magnetoencephalography source can be localized using stereo-electroencephalography information, thereby providing useful whole brain context to stereo-electroencephalography and potential role in epilepsy surgery planning.

- 1 Department of Clinical and Experimental Epilepsy, UCL, Queen Square Institute of Neurology, London WC1N 3BG, UK
- 2 Department of Neurosurgery, Ruijin Hospital, Shanghai Jiao Tong University, School of Medicine, Shanghai 200025, China
- 3 Wellcome Centre for Human Neuroimaging, UCL, Queen Square, London WC1N 3AR, UK

Correspondence to: Dr Umesh Vivekananda  
Department of Clinical and Experimental Epilepsy, Institute of Neurology,  
Queen Square, London WC1N 3BG, UK  
E-mail: u.vivekananda@ucl.ac.uk

Accepted February 27, 2021. Advance Access publication April 8, 2021

© The Author(s) (2021). Published by Oxford University Press on behalf of the Guarantors of Brain.

This is an Open Access article distributed under the terms of the Creative Commons Attribution License (<http://creativecommons.org/licenses/by/4.0/>), which permits unrestricted reuse, distribution, and reproduction in any medium, provided the original work is properly cited.

Correspondence may also be addressed to: Dr Shikun Zhan

Department of Functional Neurosurgery, Affiliated Ruijin Hospital, Shanghai Jiao Tong University, School of Medicine

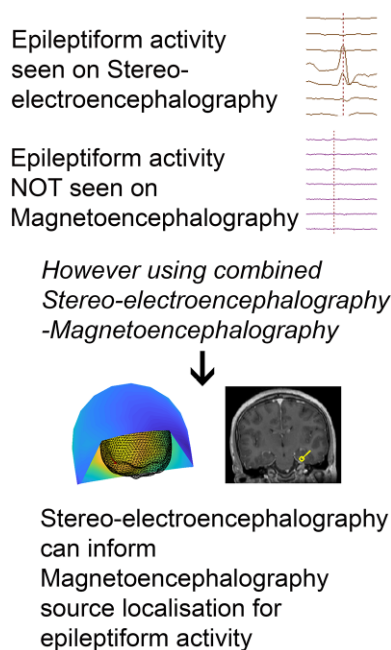
Shanghai, China

E-mail: shikun\_zhan@hotmail.com

**Keywords:** magnetoencephalography; stereo-electroencephalography; epilepsy surgery

**Abbreviations:** EZ = epileptogenic zone; MEG = magnetoencephalography; SEEG = stereo-electroencephalography

### Graphical Abstract



## Introduction

Magnetoencephalography (MEG) and stereo-electroencephalography (SEEG) can provide complementary information for the presurgical assessment of refractory focal epilepsy. MEG is non-invasive, has high temporal and spatial resolution with good global coverage, and unlike surface electroencephalography is not affected by skull conductivity.<sup>1,2</sup> However, deep sources such as the mesial temporal lobe, a region commonly associated with refractory epilepsy, are poorly detected with MEG, meaning its use in such cases is of less value.<sup>3–5</sup> This is likely because the spatial resolution decreases rapidly as a function of the depth of the epileptic generators, making source estimation challenging.<sup>6</sup> MEG is also insensitive to radially orientated sources, e.g. surface of a cortical gyrus.<sup>7</sup> It has also been shown that physiological deep brain activities can be detected using MEG if informed by SEEG,<sup>8</sup> although its relevance in a clinical context is uncertain, i.e. can MEG informed by SEEG demonstrate epileptiform activity previously not demonstrated using MEG alone.

SEEG is an invasive procedure, in which a limited set of electrodes are placed within the brain; these provide excellent detection of adjacent sources but have restricted spatial sampling. Therefore, it is difficult to interpret whether the epileptogenic zone (EZ) and SEEG electrode contacts identifying the abnormal epileptiform activity truly co-localize, or whether the zone is actually situated in nearby functionally connected brain structures. This is one of a number of reasons, including underlying pathology, age at time of surgery, and brain region where EZ was located (extra-temporal versus temporal), that surgical resection of the EZ as identified by SEEG results in a 60–70% chance of achieving seizure freedom.<sup>9</sup> MEG has previously been compared with SEEG non-concurrently, demonstrating that concordance between both modalities in identifying epileptiform activity was associated with a higher chance of seizure freedom post resection.<sup>10,11</sup> However, these studies acknowledged the limitation that MEG recordings are necessarily brief (~1 h) compared with SEEG telemetry over several days, leading to uncertainty in whether interictal activity captured by MEG and SEEG relate to identical epileptogenic foci. This is particularly relevant for scenarios where magnetic source imaging produces dispersed MEG dipoles,<sup>11</sup> which are difficult to interpret and require SEEG confirmation of the EZ. Simultaneous SEEG–MEG recording should be able to resolve such questions.

Few clinical studies on single cases have reported simultaneous SEEG and MEG recordings, most likely due to technical challenges in its acquisition.<sup>12–14</sup> We hypothesize the following; interictal activity identified by MEG and SEEG relate to the same epileptogenic focus, simultaneous SEEG–MEG can improve the identification and localization of deep brain epileptogenic sources compared to either modality alone, and removal of this source relates to good post epilepsy surgery outcome.

## Materials and methods

### Simultaneous SEEG–MEG recordings

Patients (adults and children) who underwent SEEG study for pre-surgical evaluation of drug-resistant focal epilepsy at Shanghai Jiaotong University School of Medicine during 2017 and 2019 were considered for the study. Every

**Table 1** Demographics and SEEG implantation for epilepsy patients included in study

| Case of Patient | Age (ys) | Gender | Implantation areas and<br>(number of electrode/contacts) | Pre-operative MRI                  |
|-----------------|----------|--------|--|------------------------------------|
| 1               | 47       | F      | Right T, P (4/32)  | Previous left T meningioma removal |
| 2               | 14       | F      | Right F, T, P (4/32)                                     | No abnormality                     |
| 3               | 33       | F      | Left T, P (4/32)   | Left HPC sclerosis                 |
| 4               | 18       | F      | Right F, T, and Left F and O (4/32)                      | Minimal left HPC atrophy           |
| 5               | 26       | F      | Left T, insular, O, right T (5/48)                       | No abnormality                     |
| 6               | 27       | F      | Left F, P, T (4/32)                                      | Minimal left HPC atrophy           |
| 7               | 23       | F      | Left F, T, P and Right T (5/40)                          | No abnormality                     |
| 8               | 19       | M      | Left T, P, O, and Right T, P (6/48)                      | Abnormal left P-O signal           |
| 9               | 26       | M      | Right F, T, P (4/32)                                     | No abnormality                     |
| 10              | 44       | M      | Left F, T, P (4/32)                                      | No abnormality                     |
| 11              | 9        | F      | Left T, O and Right T (6/64)                             | Abnormal left O signal             |
| 12              | 32       | M      | Left F, T and P (8/64)                                   | Left HPC sclerosis                 |
| 13              | 27       | F      | Left T, O (8/64)   | Left HPC atrophy                   |
| 14              | 12       | F      | Right F, T, P and left T (7/60)                          | No abnormality                     |

F, frontal; HPC, hippocampus; O, occipital; P, parietal; T, temporal.

patient was informed about the aim and the scope of the study and gave written informed consent. Implantation of intracranial electrodes (SDE-08: S8, S16, Beijing Sinovation Medical Technology CO., LTD, Beijing, China) was under general anaesthesia with planning guided by clinical indications, informed by prior MRI (results in Table 1), video-electroencephalography, MEG and PET studies. Of this cohort, patients who had 8 or less implanted SEEG electrodes were included for the study, due to the space constraint of the MEG helmet for simultaneous recording. Therefore, 24 patients who met this inclusion criteria were subsequently analysed. Two types of electrodes were used over the whole patient group; for electrodes with 8 contacts, the deepest contact is named as 1 and the most superficial contact named 8. For electrodes with 16 contacts, the deepest channel was named as 1 and the most superficial contact named 16. The length of contact was 2 mm, the distance between contact was 1.5 mm and the diameter of electrode was 0.8 mm.

Location and number of SEEG electrodes implanted varied between patients depending on detected epileptogenic focus (Table 1).

Simultaneous ~7 min SEEG–MEG recordings were performed with patient sitting upright using a 306-channel, whole-head VectorView MEG system (Elekta Oy, Helsinki, Finland) in a magnetically shielded room (Euroshield, Eura, Finland) situated within the hospital epilepsy unit. A clinician and scientist were present throughout the recording for patient safety. Light head bandaging was used and SEEG cap replaced if felt necessary after recording; no infection was reported in these patients. For SEEG, cable length from the head to the connectors was about 50 cm and the amplifier was powered via an isolated 24 V transformer situated in a separate electronics cabinet.

Raw MEG data were band pass filtered 0.03–330 Hz and digitized at 1000 Hz. The magnetic artefacts and movement artefact were removed by the temporal

extension of Signal Space Separation method (tSSS) implemented in the MaxFilter software (Neuromag 3.4, Elekta Oy, Helsinki, Finland). Ten patients had no epileptiform activity recorded on SEEG and so were excluded from further analysis. One patient had a seizure during recording.

SEEG analysis was performed using Brain Electrical Source Analysis software (BESA GmbH, Germany, <http://www.besa.de/> last accessed 15 April 2021), Statistical Parametric Mapping (SPM12, UCL, <https://www.fil.ion.ucl.ac.uk/spm/> last accessed 15 April 2021) and Fieldtrip (<http://fieldtriptoolbox.org> last accessed 15 April 2021). SEEG was analysed using bipolar montage (Band-pass filter 1–70 Hz, 50 Hz notch). Interictal spikes were visualized by two experts (U.V. and M.C.W) and manually marked using BESA software at the peak of maximal positive/negative deflection of the spike. The electrode contact with the largest average spike amplitude was then noted (annotated as ‘peak amplitude’ channel). Patients were then divided into superficial source and deep source groups dependent on the location of peak amplitude channel (deep: 1–3 contact number; superficial: 6–8 or 14–16 contact number). Data from all other contacts were disregarded as situated within white matter.

Locations of implanted SEEG electrodes were identified from postoperative CT scans using Lead-DBS toolbox (<https://www.lead-dbs.org/> last accessed 15 April 2021) (Figs. 1A and 3A). Post-operative CT was co-registered with a pre-operative T1 structural MRI in SPM12 and further adjusted under manual control using Slicer software (<https://www.slicer.org/> last accessed 15 April 2021). SEEG contact locations were then obtained by manually fitting electrode models to the artefacts seen in the CT, with white matter contacts rejected, using the interface implemented in Lead-DBS.

Analysis of the MEG recording was performed ‘blind’ to SEEG findings. Interictal spikes were identified using BESA software (Band-pass filter 1–35 Hz, 50 Hz notch, gain 400–800 fT). All spikes were manually marked by

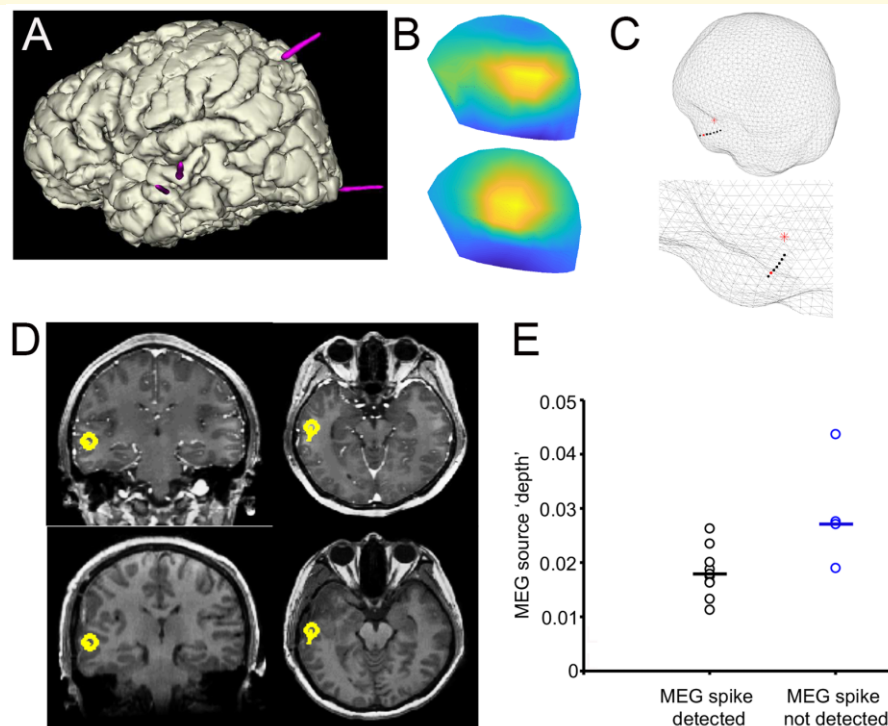


**Figure 1** Example patient with superficial epileptogenic focus (Pt 5). (A) Schematic of electrode placement. (B) Field map (measured top and modelled bottom) corresponding to the peak of the average interictal spike. (C) Relation on inner skull mesh of MEG dipole (red star) and electrode contact (red circle) with highest spike amplitude, top, and zoomed region, below. (D) Upper panel is the position of MEG dipole on pre-operative MRI scan coronal and sagittal planes; lower panel is post-operative MRI scan (E) Relationship within patients between MEG source 'depth' and presence of MEG spikes, horizontal bar indicating mean depth.

two experts (U.V. and F.R.-G.) at the peak of maximal positive deflection of the spike.

Source localization for MEG data was performed by averaging individual spikes (BESA software), before importing into SPM. A time window was then set 100 ms before the rise phase and 100 ms after the fall phase of the average spike. A single shell forward model<sup>15</sup> based on canonical meshes inverse normalized<sup>16</sup> to the pre-operative T1 structural MRI image was used, thereby creating an individual model for each patient. A single MEG dipole (Fieldtrip) was fitted and the corresponding residual variance image was also examined, in order to easily calculate distance between MEG and SEEG sources. A three dimensional co-ordinate in native space was found for both SEEG peak amplitude channel and MEG dipole, in order to calculate this distance. If there were no spikes seen on MEG alone, MEG source activity (M-source) was derived by averaging the raw MEG data informed by co-existent SEEG spikes (taken 1 s before and after highest amplitude of spike), before the same dipole fitting process was performed. This was in order to test if SEEG-MEG simultaneous recording could provide more information than visual inspection alone. To examine any relationship between 'depth' of M-source and presence of MEG spikes, we calculated the distance (d) between the

anterior commissure (AC) and dipole location in MNI space, and used  $1/d$  as an estimated measure of 'depth'. Where possible, post-resection MRI images were co-registered to the pre-operative T1 structural MRI to confirm whether M-source location was removed during surgery, and then related this to surgery outcome.

Number of spikes identified by SEEG and MEG were compared using a paired *t*-test for superficial brain sources and Mann-Whitney U-test for deep brain sources. M-source 'depth' and presence of MEG spikes was compared using *t*-test.

## Ethics approval

The study was approved by the local ethics committee of Shanghai JiaoTong University.

## Data availability

Anonymized data will be shared by request from any qualified investigator.

## Results

We first manually identified interictal spikes separately for SEEG and MEG during the simultaneous recording



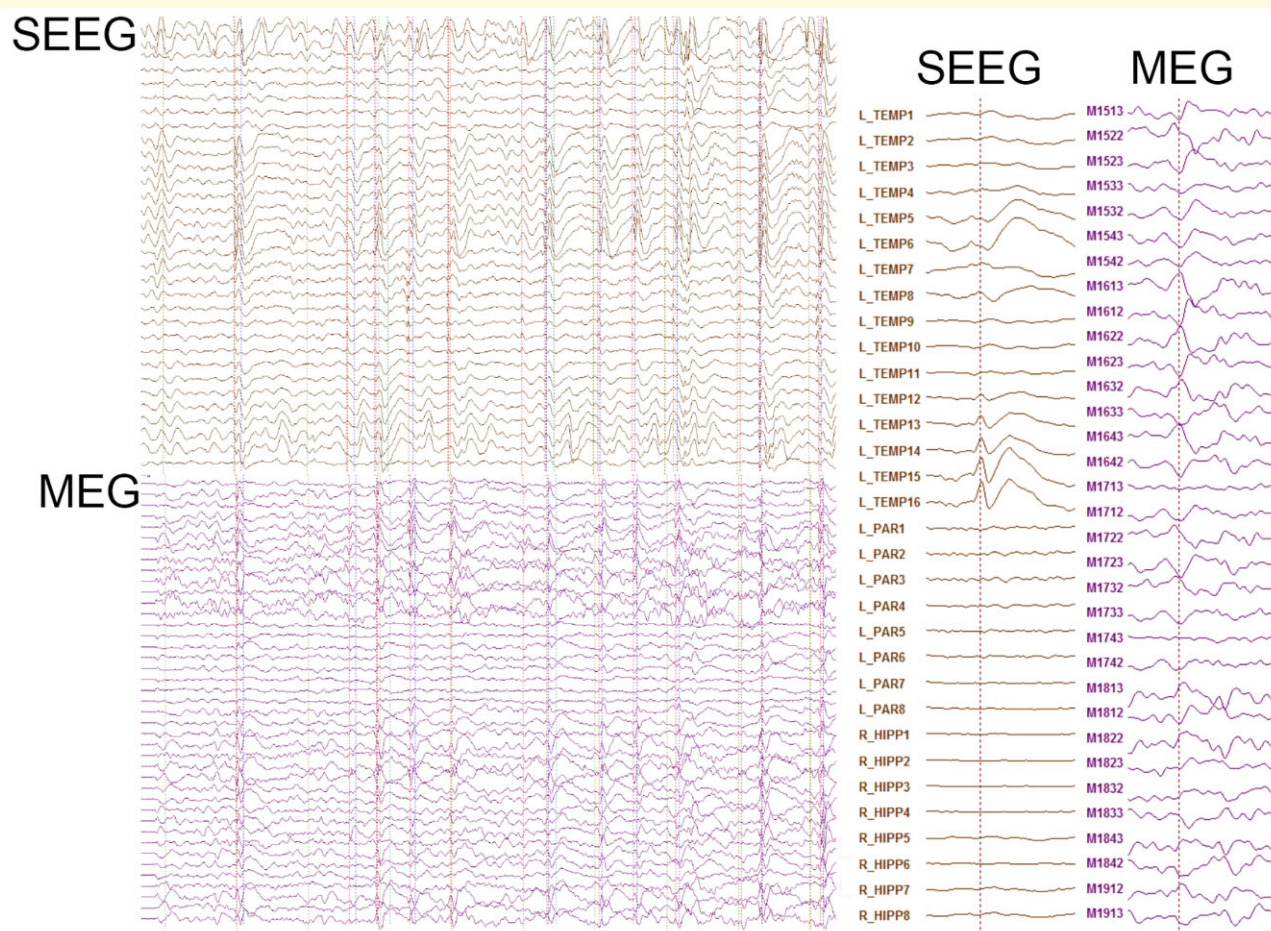


**Figure 2** Example SEEG and MEG traces from Pt 5. Raw SEEG (top) and MEG (bottom) traces with dotted lines indicating marked spikes, and magnified average SEEG and MEG interictal spike (right).

and grouped for each patient number of spikes occurring in SEEG alone, occurring concurrently in SEEG and MEG and occurring in MEG alone (Table 2). For patients whose detected epileptogenic focus was superficial cortex, as defined by the SEEG peak amplitude occurring in an electrode contact greater than four, we found no statistical difference between number of spikes identified by SEEG versus MEG (paired *t*-test,  $P=0.135$ ) (Fig. 2). This suggests that SEEG and MEG are equally sensitive in identifying interictal spikes from cortical sources. For patients with a detected deep brain epileptogenic focus defined by SEEG peak amplitude occurring in an electrode contact smaller than three, we found that number of spikes identified by SEEG was significantly higher than MEG (Mann–Whitney U-test,  $T=56.5$ ,  $P=0.002$ ) (Fig. 4), indicating that SEEG is more sensitive than MEG in identifying interictal spikes from deep sources (Table 2).

We next examined the relationship of MEG source activity (M-source) location, and location of SEEG peak amplitude channel. For patients with detected superficial

epileptogenic regions ( $n=7$ ), the mean distance between source M-source and ‘peak amplitude’ channel in native space was  $20.7 \pm 4.4$  mm. (Table 2), suggesting that location of average M-source was closely related to average SEEG interictal spike location for superficial epileptogenic regions (Fig. 1B and C). In two patients (Pt4 and 11), although SEEG identified interictal activity in the lateral temporal lobe during simultaneous recording, subsequent SEEG assessment of seizures located the seizure onset zone to be in frontal and occipital brain regions respectively. However, unlike SEEG, MEG during simultaneous recording accurately source localized to these regions (Supplementary Fig. 1).

In all superficial source patients, MEG dipole location was concordant with detected EZ on ictal SEEG and removed brain region during epilepsy surgery (Table 3), confirmed by post-operative MRI in three patients (Fig. 1D). In six out of seven cases (except patient 6), there was an Engel Class 1 outcome after 12 months.

In one patient (Pt 2), a seizure lasting 15 s was recorded. Source localization was performed on the first

**Table 2** Number of interictal spikes identified on SEEG alone, SEEG and MEG both, and MEG alone for detected superficial and deep brain sources

| Source      | Region   | Case of patient | Quantity of identified spikes |                              |           | 'Peak amplitude' channel | MEG dipole and 'peak amplitude' distance (mm) |
|-------------|----------|-----------------|-------------------------------|------------------------------|-----------|--------------------------|---|
|             |          |                 | SEEG alone                    | SEEG and MEG co-incidentally | MEG alone |                          |   |
| Superficial | Frontal  | 2               | 5                             | 18                           | 3         | Right F 6–7              | 8.10  |
|             |          | 3               | 10                            | 6                            | 0         | Left T 6–7               | 17.4  |
|             | Temporal | 4               | 4                             | 11                           | 4         | Right T 6–7              | 28.8  |
|             |          | 5               | 1                             | 14                           | 0         | Left T 10–11             | 9.09  |
|             |          | 10              | 5                             | 17                           | 3         | Left T 7–8               | 20.7  |
|             |          | 11              | 0                             | 4                            | 2         | Left T 9–10              | 42.1  |
| Deep        | Parietal | 6               | 0                             | 21                           | 0         | Left P 6–7               | 19.1  |
|             |          | 1               | 22                            | 1                            | 0         | Left HPC 2–3             | 11.3  |
|             | Temporal | 7               | 26                            | 0                            | 0         | Right HPC 1–2            | 29.8  |
|             |          | 9               | 7                             | 4                            | 1         | Left HPC 1–2             | 21.2  |
|             |          | 12              | 34                            | 0                            | 0         | Left HPC 1–2             | 8.49  |
|             |          | 13              | 26                            | 0                            | 0         | Left HPC 2–3             | 13.9  |
|             |          | 14              | 30                            | 0                            | 0         | Right HPC 2–3            | 8.40  |
|             |          | 8               | 4                             | 1                            | 0         | Left P 1–2               | 31.8  |

'Peak amplitude' channel indicates SEEG channel with highest amplitude average spike. F, frontal; HPC, hippocampus; O, occipital; P, parietal; T, temporal.

one second of high beta activity recorded at seizure onset, again using M-source and SEEG peak amplitude channel (Supplementary Fig. 2). The results were concordant with interictal findings.

For patients with detected deep epileptogenic regions ( $n=7$ ), the mean distance between M-source and 'peak amplitude' channel was  $17.8 \pm 3.7$  mm. (Table 2). In four mesial temporal cases (Pt 7,12,13,14), spikes were not visible to visual inspection on MEG, meaning that M-source was informed from SEEG spikes instead (Fig. 4). Interestingly even in these cases location of M-source was closely related to 'peak amplitude' channel location (Fig. 3B and C), suggesting that simultaneous MEG and SEEG have complementary localizing value, even in cases where no apparent MEG interictal activity is seen. There was a significant difference in MEG source depth between patients where MEG spikes were detected (mean 1/d from anterior commissure  $0.0179 \text{ mm}^{-1}$ ,  $n=10$ ) and not detected ( $0.0275 \text{ mm}^{-1}$ ,  $n=4$ ), [ $t$ -test:  $t(8) = -2.5$ ,  $P=0.027$ ; Fig. 1E].

In six out of seven patients, MEG dipole location was concordant with detected EZ on ictal SEEG and the removed brain region (Table 3), confirmed by post-operative MRI in three patients (Fig. 3D). In five out of the seven patients (except Patients 7 and 8), there was an Engel Class 1 outcome. The MEG dipole location in patient 8 (parietal lobe) was presumably outside of the resected brain region (temporal lobe), possibly explaining the persistence of seizures.

## Discussion

In the largest case series to date of epilepsy patients undergoing simultaneous SEEG-MEG study, we could

directly compare the sensitivity for both modalities in identifying interictal spikes and spike localization. Previous studies have indirectly compared MEG and SEEG,<sup>11,17</sup> with recordings performed at different time points (typically separated by a number of months) and therefore limited by variability in brain anatomy, disease status and medications taken between recordings. In addition, it is not always certain that the source of interictal activity recorded non-invasively with short-duration MEG recordings is identical to that identified using SEEG telemetry over several days. Here we could assess the same pathological epileptic brain discharges at both a local (SEEG) and global (MEG) level. We found that SEEG and MEG were comparable in identifying interictal spikes originating from superficial cortex, with MEG identifying spikes not viewed on SEEG in a number of patients. This likely reflects the relative limited spatial sampling SEEG provided. This finding however may be affected by the inherent bias that SEEG electrode placement is in part informed by prior MEG results, therefore an overlap of epileptogenic source identification between simultaneous SEEG and MEG would be expected. Average MEG dipole location was consistent with entire SEEG study findings in all superficial cases, and its removal during surgery was associated with an Engel class 1 outcome at 12 months in 6 out of 7 cases. In contrast, SEEG was superior in identifying spikes originating from key deep brain regions (e.g. mesial temporal). This has generally been perceived as a weakness of MEG both in clinical evaluation and in normal physiological studies, as it is known that spatial resolution in MEG is inversely proportional to source depth and complex deep structures such as the hippocampus can produce limited signal.<sup>18</sup> However, extracting MEG information for deep brain

epileptogenic regions is of importance as previous studies using separate SEEG and MEG recording have shown that anatomical correlation of MEG/SEEG led to a 66–85% chance of seizure freedom post epilepsy surgery compared with 11–30% when MEG/SEEG is discordant.<sup>19,20</sup>

We demonstrate a distance between average MEG dipole and peak amplitude SEEG channel of around

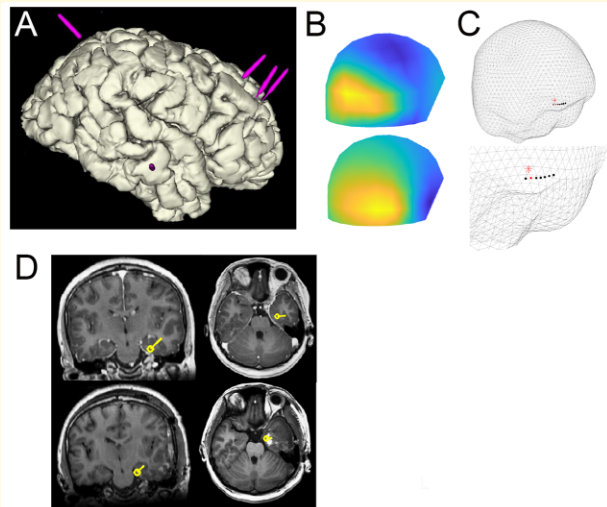


**Figure 3** Example patient with deep epileptogenic focus (Pt 14). (A) Schematic of electrode placement. (B) Field map corresponding to the peak of the average epileptic spike. (C) Relation of MEG dipole and electrode contact with highest spike amplitude. (D) Position of MEG dipole on pre-operative MRI (upper) and post-operative MRI (lower).

20 mm. for both superficial and deep epileptogenic sources. The reasons for this are probably multifactorial including propagation of interictal activity, limited spatial sampling of SEEG, and choice of MEG head model. Importantly, although spikes were not visible to visual inspection on MEG for the majority of patients with deep sources, average MEG activity informed by identified SEEG spikes still accurately localized deep source activity, which has not been demonstrated in epilepsy before. The likely reason for this finding was that averaging the MEG activity improved the low signal to noise ratio associated with deep brain activity. Our finding using a distributed inverse method commonly adopted in clinical MEG is consistent with the recent observation that SEEG informed deep brain MEG activity can be detected using independent component analysis.<sup>8</sup> This has immediate implications for the use of simultaneous SEEG–MEG recording in epilepsy surgery planning, in terms of providing MEG spatial context to SEEG ictal and interictal activity. Further work would involve performing independent component analyses on SEEG informed MEG data, in order to in future detect and localize deep source abnormal epileptiform activity not evident on visual inspection when using non-invasive MEG recording alone. Another direction would be further imaging of seizures to provide more detailed spatial information on seizure propagation, and epileptic networks involved. We further show that surgical resection of the consequent average MEG dipole predicted seizure freedom at 12 months (5 out of 6 patients); the one patient where the dipole was not removed had seizure recurrence. However, more subjects would be required to properly assess the utility of SEEG–MEG recordings in predicting outcome post epilepsy surgery.

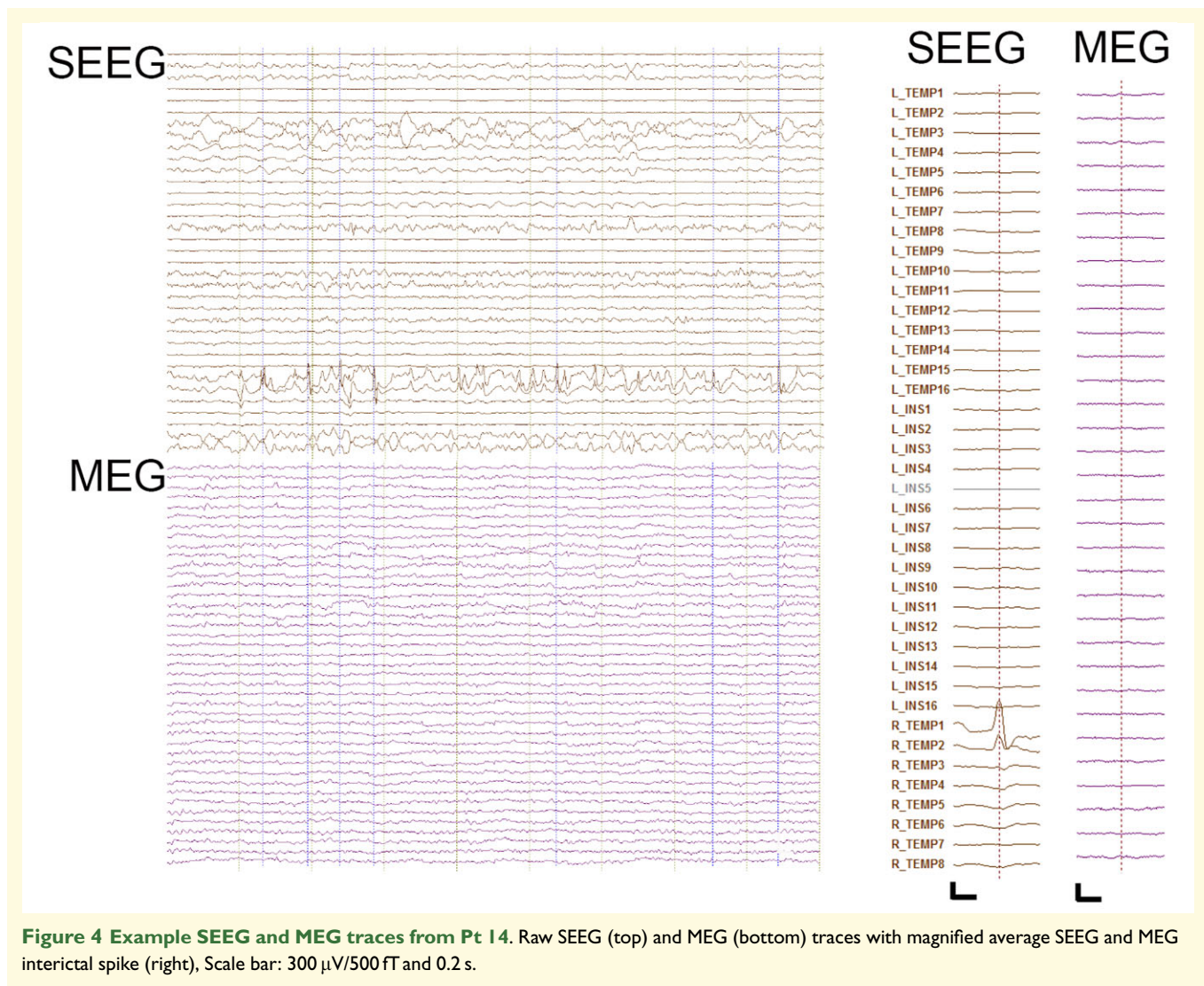
**Table 3** Post surgery outcomes after 1 year

| Patient | SEEG (entire recording)             | SEEG (simultaneous recording) | MEG dipole     | Source location                | Resection                             | Engel class |
|---------|-------------------------------------|-------------------------------|----------------|--------------------------------|---------------------------------------|-------------|
| 1       | Left F and mesial T                 | Left mesial T                 | Left mesial T  | Deep—HPC                       | Left T resection                      | I           |
| 2       | Right F                             | Right F                       | Right F        | Superficial—insular            | Right F, insular, operculum resection | I           |
| 3       | Left T                              | Left T                        | Left T         | Superficial—temporal neocortex | Left T resection                      | I           |
| 4       | Left F                              | Right T                       | Left F         | Superficial—superior frontal   | Right F resection                     | I           |
| 5       | Left T                              | Left T                        | Left T         | Superficial—temporal neocortex | Left T resection                      | I           |
| 6       | Left P                              | Left P                        | Left P         | Superficial—parietal cortex    | Left P resection                      | II          |
| 7       | Bilateral mesial T—left predominant | Right mesial T                | Right mesial T | Deep—HPC                       | Left T resection                      | II          |
| 8       | Left T and P                        | Left P                        | Left P         | Deep—parietal                  | Left T resection                      | II          |
| 9       | Left T and P                        | Left mesial T                 | Left P         | Deep—parietal                  | Left P resection                      | I           |
| 10      | Right T                             | Right mesial T                | Right T        | Superficial—temporal neocortex | Right T resection                     | I           |
| 11      | Left T                              | Left T                        | Left T         | Superficial—temporal neocortex | Left O resection                      | I           |
| 12      | Left HPC                            | Left mesial T                 | Left mesial T  | Deep—HPC                       | Left T resection                      | I           |
| 13      | Left mesial T                       | Left mesial T                 | Left mesial T  | Deep—HPC                       | Left T resection                      | I           |
| 14      | Right mesial T                      | Right mesial T                | Right mesial T | Deep—HPC                       | Right T resection                     | I           |

SEEG entire recording describes location derived from prolonged telemetry and SEEG simultaneous recording describes location derived from simultaneous SEEG/MEG recording.

F, frontal; HPC, hippocampus; O, occipital; P, parietal; T, temporal.





There were limitations of the study, including the brevity of recordings and consequently the limited number of cases analysed, which was dictated by the technical difficulty of acquiring simultaneous SEEG and MEG data. Secondly, due to the size constraint of the MEG helmet, patients selected for simultaneous recording had a maximum of 8 implanted SEEG electrodes. Therefore, the relatively low SEEG coverage may have influenced direct comparison of SEEG to MEG for detection of spikes. However, one may argue that denser SEEG coverage would have further improved SEEG informed MEG deep brain activity localization due to increased information. Further development of this method would involve longer recording times and accommodation of larger SEEG implantation schemes when recording MEG.

Simultaneous SEEG and MEG can thus provide complementary information about the spatial extent of interictal epileptiform activity, in particular for deep epileptogenic sources, and so better inform resection planning.

## Supplementary material

Supplementary material is available at *Brain Communications* online.

## Acknowledgements

We would like to thank all the patients who took part in this study. We would like to thank Andreas Horn and Ningfei Li for their help with adding support for SEEG electrode reconstruction to Lead-DBS.

## Funding

U.V. is funded by National Institute of Health Research, Epilepsy Research UK (P1906), Medical Research Council (MR/T033150/1) and Academy Medical Sciences

(SGL021\1002). V.L. is funded by Wellcome Trust. C.C. is funded by National Natural Science Foundation of China.

## Competing interests

All authors report no conflicts of interest.

## References

1. Plummer C, Vogrin SJ, Woods WP, Murphy MA, Cook MJ, Liley DTJ. Interictal and ictal source localization for epilepsy surgery using high-density EEG with MEG: A prospective long-term study. *Brain*. 2019;142(4):932–951.
2. Rampp S, Stefan H, Wu X, et al. Magnetoencephalography for epileptic focus localization in a series of 1000 cases. *Brain J Neurol*. 2019;142(10):3059–3071.
3. Guy CN, Walker S, Alarcon G, et al. MEG and EEG in epilepsy: Is there a difference? *Physiol Meas*. 1993;14 (Suppl 4A): A99–A102.
4. Hillebrand A, Barnes GR. A quantitative assessment of the sensitivity of whole-head MEG to activity in the adult human cortex. *NeuroImage*. 2002;16(3, Part A):638–650.
5. Stephen JM, Ranken DM, Aine CJ, Weisend MP, Shih JJ. Differentiability of simulated MEG hippocampal, medial temporal and neocortical temporal epileptic spike activity. *J Clin Neurophysiol*. 2005;22(6):388–401.
6. Wennberg R, Valiante T, Cheyne D. EEG and MEG in mesial temporal lobe epilepsy: Where do the spikes really come from? *Clin Neurophysiol*. 2011;122(7):1295–1313.
7. Hämäläinen M, Hari R, Ilmoniemi RJ, Knuutila J, Lounasmaa OV. Magnetoencephalography—Theory, instrumentation, and applications to noninvasive studies of the working human brain. *Rev Mod Phys*. 1993;65(2):413–497.
8. Pizzo F, Roehri N, Villalon SM, et al. Deep brain activities can be detected with magnetoencephalography. *Nat Commun*. 2019; 10(1):1–13.
9. de Tisi J, Bell GS, Peacock JL, et al. The long-term outcome of adult epilepsy surgery, patterns of seizure remission, and relapse: A cohort study. *Lancet Lond Engl*. 2011;378(9800):1388–1395.
10. Knowlton RC, Elgavish R, Howell J, et al. Magnetic source imaging versus intracranial electroencephalogram in epilepsy surgery: A prospective study. *Ann Neurol*. 2006;59(5):835–842.
11. Murakami H, Wang ZI, Marshly A, et al. Correlating magnetoencephalography to stereo-electroencephalography in patients undergoing epilepsy surgery. *Brain*. 2016;139(11):2935–2947.
12. Gavaret M, Dubarry A-S, Carron R, Bartolomei F, Trébucqon A, Bénar C-G. Simultaneous SEEG-MEG-EEG recordings overcome the SEEG limited spatial sampling. *Epilepsy Res*. 2016; 128:68–72.
13. Badier JM, Dubarry AS, Gavaret M, et al. Technical solutions for simultaneous MEG and SEEG recordings: Towards routine clinical use. *Physiol Meas*. 2017;38(10):N118–N127.
14. Santiuste M, Nowak R, Russi A, et al. Simultaneous magnetoencephalography and intracranial EEG registration: Technical and clinical aspects. *J Clin Neurophysiol*. 2008;25(6):331–339.
15. Nolte G. The magnetic lead field theorem in the quasi-static approximation and its use for magnetoencephalography forward calculation in realistic volume conductors. *Phys Med Biol*. 2003; 48(22):3637–3652.
16. Mattout J, Henson RN, Friston KJ. Canonical source reconstruction for MEG. *Comput Intell Neurosci*. 2007;2007:67613.
17. Cohen D, Cuffin BN, Yunokuchi K, et al. MEG versus EEG localization test using implanted sources in the human brain. *Ann Neurol*. 1990;28(6):811–817.
18. Attal Y, Schwartz D. Assessment of subcortical source localization using deep brain activity imaging model with minimum norm operators: A MEG study. *PLoS One*. 2013;8(3):e59856.
19. Almubarak S, Alexopoulos A, Von-Podewils F, et al. The correlation of magnetoencephalography to intracranial EEG in localizing the epileptogenic zone: A study of the surgical resection outcome. *Epilepsy Res*. 2014;108(9):1581–1590.
20. Schneider F, Alexopoulos AV, Wang Z, et al. Magnetic source imaging in non-lesional neocortical epilepsy: Additional value and comparison with ICEEG. *Epilepsy Behav*. 2012;24(2):234–240.